SSRG International Journal of Civil Engineering
ISSN: 2348-8352/ https://doi.org/10.14445/23488352/IJCE-V12I3P115

Volume 12 Issue 3, 162-175, March 2025
© 2025 Seventh Sense Research Group®

Original Article

Geospatial Evaluation of Soil Degradation in Western Himalayan Basins; A Case Study for Alaknanda Basin

Nyigam Bole[1], Kedovito Chasie[2], Munuvelu Vese[3], Arnab Bandyopadhyay[4], Aditi Bhadra[5]

[1,2,3,4,5]*Department of Agricultural Engineering NERIST, Nirjuli, Arunachal Pradesh, India.*

[1]*Corresponding Author : pudruksh@gmail.com*

Received: 12 January 2025 Revised: 11 February 2025 Accepted: 09 March 2025 Published: 29 March 2025

Abstract - *To implement effective conservation plans, it is crucial for policymakers first to evaluate the extent of soil deterioration within the designated region to develop more targeted and impactful measures. The soil erosion model (RUSLE) incorporated with geospatial techniques was used to examine soil loss in high altitude Alaknanda River basin, situated in the Uttarakhand, Chamoli district in the Western Himalayas for a fifteen-year period (2004–2018). The estimated soil depletion was categorized into six distinct levels of erosion vulnerability, spanning from minimal to extremely high-risk classes. The study highlights the significant vulnerability of the Alaknanda River basin to soil loss, having an anticipated average loss of 28.45 t ha−1 yr−1, surpassing the permissible limit of 25 t ha−1 yr−1 in young mountain environments. The majority of the eroded portion is categorized within the slight erosion class at 43.67%, and the minority of the eroded region falls under the medium erosion class at 3.78%. The overall temporal variation in mean soil loss shows a rising pattern from 2004 to 2010, followed by a decrease from 2010 to 2018, following a pattern like that of the Ṛ-factor temporal trend, which also increases from 2004 to 2010 and decreases thereafter, underscoring the significant influence of rainfall on soil loss in Alaknanda. This geospatial evaluation of soil degradation in the Alaknanda basin offers valuable perspectives on the underlying factors resulting in erosion and pinpoints key areas that warrant priority interventions.*

Keywords - *Alaknanda, GIS, RUSLE, Soil degradation, Spatio-temporal variation.*

1. Introduction

Sedimentation is a global phenomenon that degrades agricultural land by removing surface soil rich in nutrients, increasing runoff from very low permeable subsoil, and reducing the amount of water available to plants. Hence, the success of a soil conservation program hinges on accurately calculating soil loss and pinpointing critical areas where optimal management practices should be implemented. Numerous field-based studies carried out in various places and river basins have shown that soil erosion rates in India's Himalayas are exceptionally high. Given the potential for climate shift and the correlated fluxes in precipitation intensities, it is expected that these erosion rates would increase.

The non-uniformity of soil erosion rates worldwide results from significant temporal and geographical variations in erosion processes. These variations depend on factors such as temperature fluctuations, topographical features, land use, and human activity. Areas with undulating landscapes, agricultural land, sub-humid regions, semi-arid land, and dry land are particularly erosion-sensitive. [7] Given the challenging geographical and topographic conditions in the higher Himalayan regions, field-based surveys and investigations have their limitations. Consequently, RS and GIS techniques play a pivot role in offering viable solutions and enhancing our comprehension of hydrological processes on a regional scale in the Himalayas. Due to the challenges and limitations of conducting extensive measurements of soil erosion rates across large areas, it is vital to employ various soil erosion models.

Researchers have applied these models—which fall into the empirical, semi-empirical, and physical/process-based categories-in various ways. They vary in terms of the processes they incorporate, their level of complexity, and their data requirements, making them valuable tools for forecasting soil erosion rates across various scales providing valuable insights for effective land management strategies. [9] One distinctive feature of the Revised Universal Soil Loss Equation (RUSLE) model is its widespread acceptance and popularity for evaluating erosion risk at many scales, including watersheds [12, 17] catchments and local levels. [15] Though there are a number of effective soil erosion models, such as the Water Erosion Prediction Project (WEPP), Modified Universal Soil Loss Equation (MUSLE), Environmental Policy Integrated Climate (EPIC), etc., the RUSLE model was selected for this study as the model is

This is an open access article under the CC BY-NC-ND license (http://creativecommons.org/licenses/by-nc-nd/4.0/)

highly efficient and requires minimal data to estimate soil erosion, especially in the mountainous ungauged basin. Integrating with Remote Sensing (RS) and GIS platforms enhances and streamlines the overall analysis. Although RUSLE does not predict sediment transport, it effectively estimates soil loss and can calculate sediment yield when combined with Sediment Delivery Ratio (SDR) models. Additionally, it prioritises erosion risk and facilitates the analysis of temporal changes. The advancement in geospatial techniques RS and GIS methodologies, along with their growing accessibility, has significantly improved the cost-effectiveness, accuracy, and application scope for estimating both the quantity and spatial dispersion of soil degradation [2].

The study region comprises vast areas of snow-covered and barren land with minimal green canopy; therefore, with climate change accelerating snowmelt, the resulting increase in overland and channel flow heightens soil vulnerability to erosion. The region has also experienced frequent natural events like flash floods and lake glacier outbursts leading to landslides, consequently degrading the soil structure. [20] According to a study conducted by Sharda & Ojasvi, [19] out of the total sediment contribution from India, 81% is contributed from the reservoirs located in North India regions.

While recent studies have assessed soil erosion at the state level, there has been a lack of prioritization for soil erosion studies in the area, and no assessment of temporal variations has been conducted. Understanding these changes and the rate at which they change over time is crucial for developing effective mitigation actions to decrease the hazardous impacts of soil erosion. This study employs a GIS framework and integrates multiple remote sensing inputs to apply RUSLE to determine soil degradation in the Alaknanda basin. The study's main objectives include classifying the basin into different soil erosion risk classes and examining temporal trends in soil degradation patterns.

2. Data and Methodology

2.1. Study Region

Alaknanda basin of Chamoli district, Uttarakhand state, in the western Himalayan region, spans from 30.5° N up to 31° N and 78.75° E to 80° E, covering 10,882 square kilometers area. This region exhibits a wide altitudinal range, from 1,414 meters to 7,736 meters. The topography is characterized by steep terrain, deep canyons, and river valleys.

The basin is divided into four primary sections: the Great Himalayan Range, the Middle Himalaya, the Alpine and grazing areas, and the river valleys. The Alaknanda River watershed has a dendritic drainage system. Rainfall in this region ranges from 600 to 1200 mm annually, and the climate is subtropical to alpine. Millions of people in the watershed and downstream depend on this basin for their lives, which has a major impact on the Ganga River's hydrology. The region experiences heavy snowfall during the winter season, with maximum snow cover observed in March, gradually depleting until seasonal snow accumulation begins in October. For this study, the Alaknanda basin was delineated at an outlet point located at 30° 33’ 57” N and 79°32’ 57” E coordinates. A total basin area of 4561.54 square kilometers is encompassed in the study region (Figure 1).

2.2. Acquisition of Data

By utilizing the "RUSLE" soil erosion model's fusion of RS and GIS, the assessment of soil loss entails the gathering of diverse data types. This methodology not only facilitates the estimation and measurement of soil erosion and its risk, but it also enables the analysis of the temporal variations across diverse locations and timeframes. Incorporating RS and GIS technology empowers the efficient collection and management of vast datasets essential for comprehensive studies in this field.

The following datasets of spatial, meteorological and Moderate Resolution Imaging Spectroradiometer (MODIS) images have been used for this research. Table 1 provides the different datasets utilized for the analysis.

2.2.1. Spatial Data

SRTM Digital Elevation Model (DEM) engulfing the Alaknanda River basin, with 30 meters × 30 meter resolution, was downloaded from the website https://dwtkns.com/srtm30m/. The required soil map for the state was obtained from ICAR-NBSS&LUP (https://nbsslup.icar.gov.in/). And Land Use Land Cover (LULC) data was procured from https://daac.ornl.gov/get_data/.

Table 1. Data inputs for the study

Sl. No	Factor	Data	Duration
1	Rainfall Erosivity (R-factor)	CPC (0.5°×0.5°)	2004 – 2018 (Daily Precipitation)
2	Soil Erodibility (K-factor)	1. ICAR-NBSS & LUP soil map (1:250000) 2. Soil grid (250m)	-
3	Topography (LS-factor)	SRTM DEM (30m)	-
4	Cover management (C-factor)	MOD13Q1 (250m)	2004 – 2018 (images with 16 days interval)
5	Support Practice (P-factor)	ORNL DAAC LULC (100 m)	2005

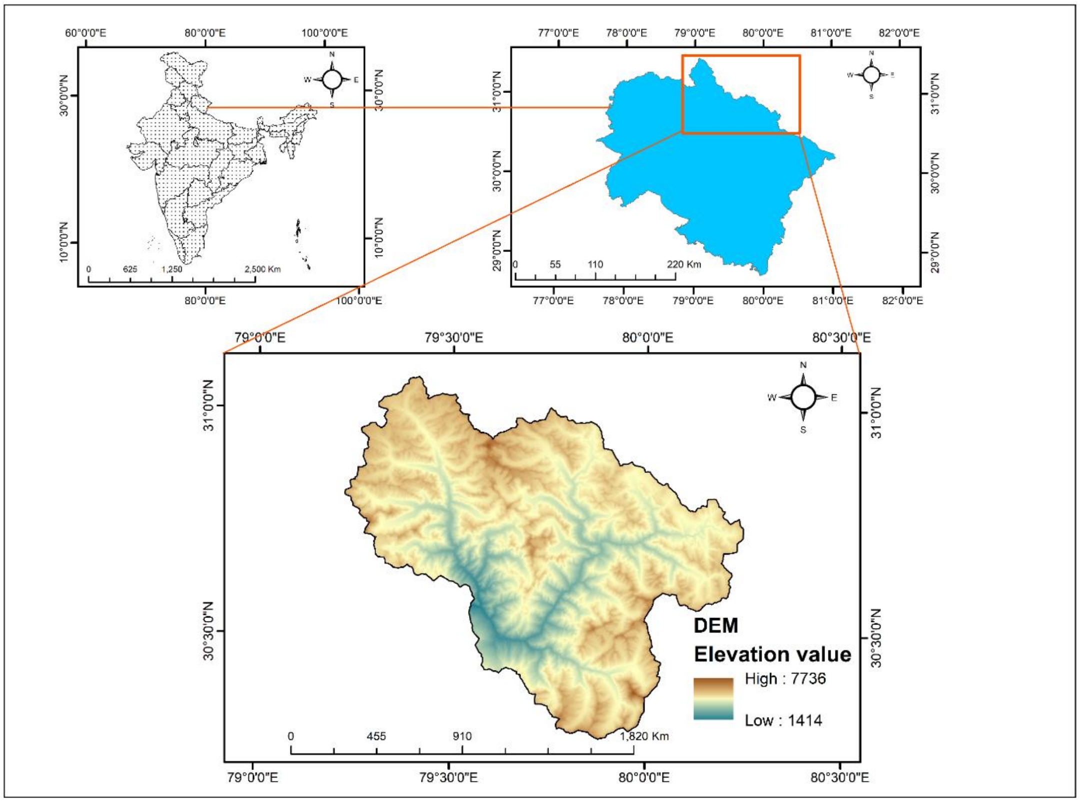

Fig. 1 Position of the study region, alaknanda basin

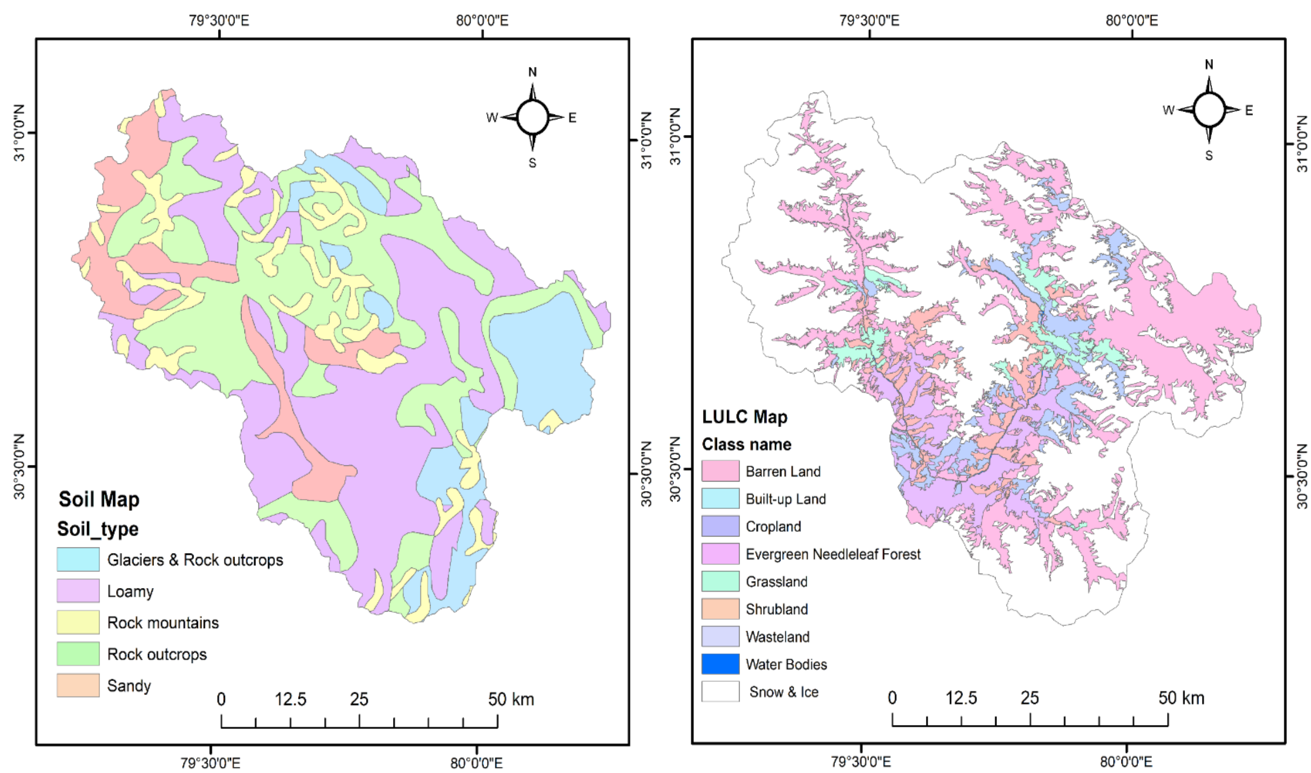

Fig. 2 Soil map and LULC map of alaknanda basin

2.2.2. Meteorological Data

The meteorological (precipitation) data of the Alaknanda River basin for 15 years, i.e., 2004-2018, was collected from Climate Prediction Centre (CPC) data https://psl.noaa.gov. While ground observed data from multiple stations in the region could be more beneficial for use in the study, due to limited data recording stations, the current gridded precipitation data was considered considering its temporal and spatial coverage.

2.2.3. MODIS Normalized Difference Vegetation Index Product

The acquisition of MOD13Q1 16-Day tile data, encompassing a 250m resolution over a 15-year period (2004 – 2018), specifically for the Alaknanda River basin in Uttarakhand, forms a pivotal component of this study. The dataset of MODIS or Terra Vegetation (MOD13Q1) Indices of 16-Day interval L3 Global 250m product serves the purpose of providing pseudo-colored, 16-day composite Vegetation Indices. The utilization of this dataset contributes to reliable comparisons of vegetation conditions, ensuring a comprehensive analysis of spatio-temporal scales in the study region.

2.3. Pre-processing of Spatial Data

DEM, MODIS NDVI, LULC map and Soil map were pre-processed using Arcmap 10.5 with the required available tools within the environment. Reprojection to WGS 1984 UTM zone 44N and resampling of Soil map, LULC map and MODIS NDVI to DEM resolution (30m) resolution were performed. Figure 2 shows the LULC map and Soil map of the Alaknanda basin.

2.4. RUSLE Model for Mean Annual Soil Loss Evaluation

Researchers from various countries have widely acknowledged and applied the RUSLE model at the regional scale, attesting to its broad recognition in soil degradation studies [15, 25] representing diverse topographic conditions. This evaluation of the annual mean soil degradation amount in the Alaknanda basin serves the objective of identification and prioritization in the study of soil degradation patterns. The average yearly soil loss value was computed employing Equation (1).

$$A = R \times K \times LS \times C \times P \qquad (1)$$

In the given Equation (1), ‘A’ represents the yearly loss os soil for a unit area (measured in t ha−1 yr−1), with its estimation influenced by factors such as ‘Ŗ’ (erosivity factor of rainfall), ‘LS’ (length of slope and slope steepness factor), ‘κ’ (erodibility factor of soil), ‘P’ (conservation practice factor, ranging within 0 and 1), and ‘C’ (factor associated with managing of land).

2.4.1. Determination of Ŗ-Factor

Rainfall erosivity is identified as the amount of kinetic energy produced when rain hits the ground, which affects the rate of runoff. The value of Ŗ and the quantity and intensity of rainfall appear to be directly correlated, meaning that higher precipitation levels translate into higher Ŗ values. The Ŗ factor value for each month over fifteen years was determined using the connection Arnoldus has given (Equation (2)) [1].

$$Ŗ = \sum_{i=1}^{12} 1.735 \times 10^{\left(1.5 \log 10 \left(\frac{P_i^2}{P}\right) - 0.08188\right)} \qquad (2)$$

Ŗ = erosivity of rainfall (MJ mm ha-1 h-1 y-1)
P_i = sum of rainfall for i^{th} month (mm)
P = sum of rainfall in a year (mm)

2.4.2. Determination of κ-Factor

This factor contributes a crucial part by encapsulating the influence of rainfall, infiltration, and runoff on soil degradation. It includes the influence of soil characteristics, particularly during storm events in elevated terrains, providing a comprehensive assessment of soil degradation factors. [18] This factor is commonly calculated using experimental equations or corresponding nomographs to capture the intricate relationships between soil properties, rainfall, infiltration, and runoff. [26] By utilizing observed soil parameters such as texture, structural characteristics, permeability class, and organic content, the soil erodibility factor can be calculated. This approach enables a quantitative assessment of this factor grounded on the specific attributes of the soil under consideration in accordance with Equation (3).

$$K = 2.8 \times \frac{1}{10^7} \times M^{1.14} \times (12 - a) + 4.3 \times \frac{1}{10^3} \times (b - 2) + 3.3 \times \frac{1}{10^3} \times (c - 3) \qquad (3)$$

Where κ = soil erodibility factor (t ha h ha-1 MJ-1 mm-1)
M = Particle size distribution (very fine sand % + silt %) × (100 – clay %)
a = concentration of organic matter (%)
b = soil structure code (dimensionless)
c = permeability class/code (dimensionless)

The soil parameters of ‘M’, ‘b’ and ‘c’ of each soil type were allocated with values in accordance with the National Soils Handbook No. 430. [22] As there was no soil sample collected for the study region, the value of 'a' was obtained from ‘Soilgrid250m’ at https://soilgrids.org/ with an interval depth of 0 – 30 cm. Raster map for each of the soil parameters were prepared and resampled to the cell size of DEM to calculate K factor.

2.4.3. Determination of LS-Factor

The fraction of soil loss from a particular land parcel having a defined slope and gradient distance to a standardized plot is measured by the LS factor. The standard plot is defined with a slope of 9 % and a unit plot length of 22.13 meters while keeping all the other soil conditions constant. The equation selected for this study for LS factor calculation was first published by Moore and Burch and has undergone some minor changes. [13] The expression used for obtaining the LS factor is as follows (see Equation (4)):

$$LS = \left[\frac{Flow\ accumulation\ \times cellsize}{22.1}\right]^{1.4} \times \left(\frac{\sin(slope \times 0.01745)}{0.09}\right)^{1.4} \times 1.4 \quad (4)$$

LS = slope length and steepness
flow accumulation = total area adding to an upstream of a specific location on a terrain.
cell size = 30 m (DEM resolution)
slope = slope map in degree

2.4.4. Determination of C-Factor

It is a crucial parameter in erosion estimation. It compares soil eroded from a particular region under particular cropping conditions to the same area eroded and managed with well-cultivated and fallow practices. The C-factor makes evaluating how different land governance techniques affect soil loss easier. To calculate the crop management factors (C-values), Equation (5) was used, which included the Normalized Difference Vegetation Index (NDVI) [24].

$$Ç = exp\left[-a\frac{NDVI}{b-NDVI}\right] \quad (5)$$

Where α a = 2 and ß b = 1 are scalar coefficient factors that define the curve shape describing the relationship between Ç parameter and vegetation index (NDVI). The study calculated the mean Ç values for each year and visualized their temporal changes by plotting them against the corresponding years.

2.4.5. Determination of P-Factor

This factor assesses the efficacy of soil protection methods in mitigating erosion compared to conventional tillage and cultivation on slopes. It considers practices like contouring, strip cropping, and terracing influencing runoff velocity, concentration, and drainage patterns. These values are calculated based on slope, land use condition and their oversight practices.

In order to make this change in the current work, the P factor was kept as 1 for the land cover classes and 0 for the areas with snow cover and no data. Having resampled all computed factors to a uniform resolution of 30m, soil erosion mapping facilitated a spatio-temporal analysis of soil erosion within the catchment.

2.5. Spatio-Temporal Variation in Yearly Mean Soil

The raster-based maps, illustrating the estimated soil erosion spanning a fifteen-year period from 2004 to 2018 in the basin, were subsequently classified into six priority classes. The purpose of these classes was to map out the study region's mean soil erosion's geographic distribution. Low, Medium, High, Very High, Severe, and Very Severe are the categories for soil erosion risk, and the range of loss values for the same in t ha^{-1} yr^{-1} is 0 – 5, 5 – 10, 10 – 20, 20 – 40, 40 – 80, and > 80 respectively according to the classification system given by Singh et al., [20] for the requirements of India serving as the basis for this study [11, 16].

In order to analyze the temporal fluctuation in soil loss, a thorough evaluation was conducted by examining the annual mean soil erosion values per year within the designated timeframe, which ran from 2004 to 2018, throughout the whole study area. This systematic examination aimed to discern fluctuations and patterns in soil erosion dynamics over the fifteen-year period, which were mainly attributed to rainfall erosivity and cover management factors. By scrutinizing the annual variations, researchers could identify trends, anomalies, or significant alterations in the degree of soil degradation across the basin area.

3. Results and Discussion

3.1. RUSLE Factors

3.1.1. Rainfall Erosivity Factor

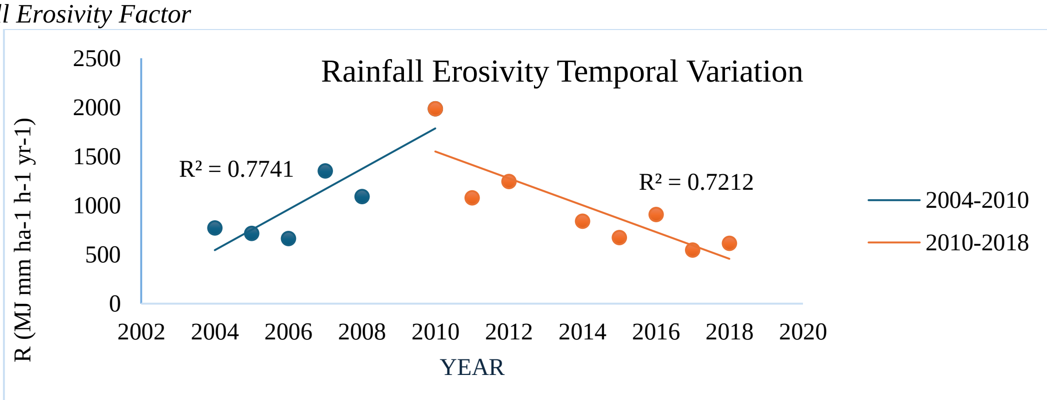

Fig. 3 Temporal variation in R-factor for the study period (2004-2018)

Table 2. Annual rainfall erosivity factor (Ŗ) values for fifteen years window

Year	Ŗ factor (MJ mm ha^{-1} h^{-1} yr^{-1})
2004	769.803
2005	715.6008
2006	663.7894
2007	1350.814
2008	1090.574
2009	447.061
2010	1985.522
2011	1077.551
2012	1242.613
2013	1777.45
2014	838.531
2015	673.752
2016	908.279
2017	546.331
2018	613.788
Average	**978.985**

Ŗ-factor analysis within the Upper Alaknanda River basin over the 15-year period from 2004 to 2018 revealed a range of values spanning from 447.061 to 1985.522 MJ mm ha-1 h-1 y-1, garnering an average value of 978.985 MJ mm ha-1 h-1 y-1. Notably, 2009 exhibited the lowest Ŗ-factor value, while the peak value was recorded in 2010 (Table 2). The Ŗ-factor is affected by factors such as rainfall duration, duration, and total amount, leading to fluctuations throughout the year. The high Ŗ-factor value could be attributed to possibly high recorded rainfall in 2010. A closer examination of the temporal fluctuation in the R-factor, when plotted against the mean Ŗ-value across consecutive years, disclosed an increasing trend from 2004 to 2010. Subsequently, from 2010 to 2018, a decreasing trend was observed (Figure 3). This temporal analysis not only provides a snapshot of the variability in rainfall erosivity but also suggests distinct periods of increase and decrease, emphasizing the dynamic nature of erosive forces within the Upper Alaknanda River basin during the specified timeframe. Understanding these trends is imperative for formulating efficient soil protection and land management strategies in response to changing erosive conditions.

3.1.2. Soil Erodibility Factor

The value of the parameters has been assigned for each soil type as per the US Department of Agriculture (USDA) literature based on the soil map (Table 3). The estimated κ-factor in the Alaknanda basin ranges from 0.0 to 0.129, having a mean value of 0.031 in t ha h ha-1 MJ-1 mm-1. With a mean value of 0.0654 t ha h ha-1 MJ-1 mm-1, sandy soil had the highest erodibility factor. Table 4 records the κ values for different various types of soil. The κ-factor and its parameters' spatial distribution map are displayed in Figure 4. This data offers a thorough grasp of the basin's κ-factor variability, enabling focused conservation initiatives and environmentally friendly behaviours. Identifying specific soil types, such as sandy soil with elevated erodibility values, becomes crucial for implementing mitigation strategies and safeguarding against soil erosion in vulnerable regions.

Table 3. Soil erodibility factor parameters (particle size parameter, permeability class and soil structure class)

Soil Type	Particle size Parameter (M)	Permeability Class (c)	Soil Structure Class (b)
Sandy	9192.28	1 (rapid)	3
Loamy	7225	3 (moderate)	2
Glaciers & Rock Outcrops	0	0	0
Rock Mountains	0	0	4
Rock Outcrops	0	6 (very slow)	4

3.1.3. Topography Factor

This is a critical parameter reflecting the topographic characteristics of the Alaknanda River basin, exhibiting a wide range, spanning from <1.00 up to 1,437.89. The average LS factor for the entire basin was determined as 3.915, having a standard deviation of 9.332. Most of the portion of the basin falls under the LS-factor value ranging within < 1 to 10, and few pixels having LS-factor value ranging from 10 – 30 were observed in regions particularly with steeper slopes, whereas very few pixels were found with LS-factor value higher than 30 as shown in Figure 5. Notably, certain regions within the basin experience notably high slope erosion, contributing to the variability observed in the LS factor values. These elevated slope erosion areas underscore topography's significance in influencing soil loss dynamics. In areas where slope erosion is a serious risk to soil stability and ecosystem health, the spatial variation offers important information for setting conservation priorities and putting targeted land management strategies into practice. Recognizing and addressing these differences in slope factors are fundamental for devising efficient erosion control strategies customized to the unique conditions within the basin.

3.1.4 Cover Management Factor (CMF)

CMF analysis assessment was omitted in areas covered with snow and ice due to the lack or minimal presence of vegetative cover in those regions. The Ç-factor spatial distribution obtained by Singh and Kansal [21] study mirrors a comparable pattern to the current study, with the north and eastern regions being dominated by higher Ç values (Figure 6). The temporal analysis of the Ç value within the specified period revealed notable variations, with the maximum mean Ç value observed in the year 2005 at 0.67 and the lowest mean Ç value of 0.55 obtained in the year 2016. The overall average Ç value for the entire basin was calculated to be 0.63. When examining the trend over consecutive years and plotting the mean Ç values, a subtle but discernible decreasing pattern emerged. This trend signifies a gradual decline in the CMF over the specified time frame. Recognizing the temporal dynamics of the C-value is pivotal for evaluating changes in land use, vegetation, and their influence on soil degradation. The observed trend may prompt further investigation into factors influencing land cover changes and guide the implementation of conservation strategies aimed at maintaining or enhancing cover management within the basin.

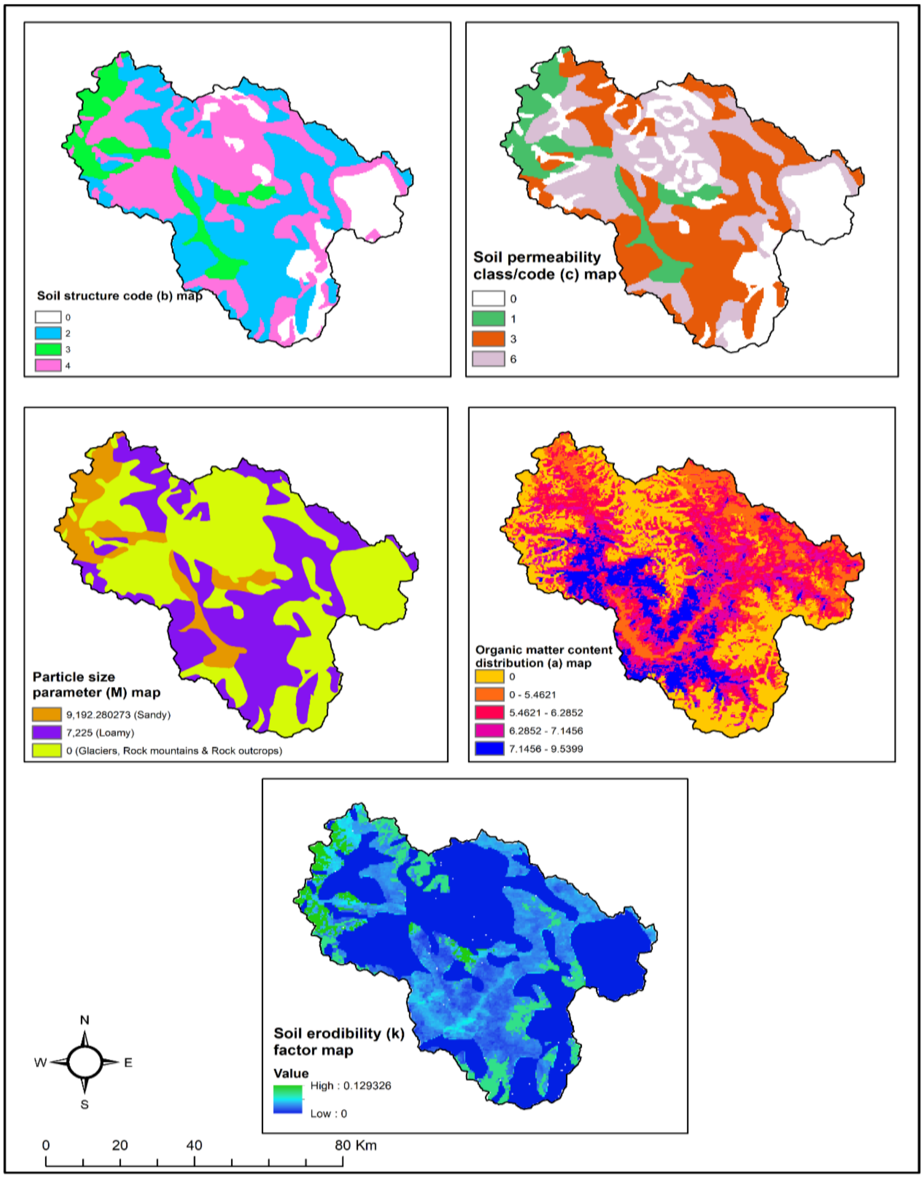

Fig. 4 Soil structure code (b), Soil permeability code (c), Organic matter content (a), Particle size parameter (M), and K-factor map.

Table 4. κ -factor for various soil types of the Alaknanda River basin

Soil Type	Area (km^2)	Percentage (%)	Average k -factor
Sandy	569.81	10.75	0.0654
Loamy	484.77	37.31	0.0488
Glaciers & Rock outcrops	1683.06	12.63	0.0008
Rock mountains	470.14	10.42	0.003
Rock outcrops	1303.08	28.89	0.0195
Total	**4510.86**	**100**	

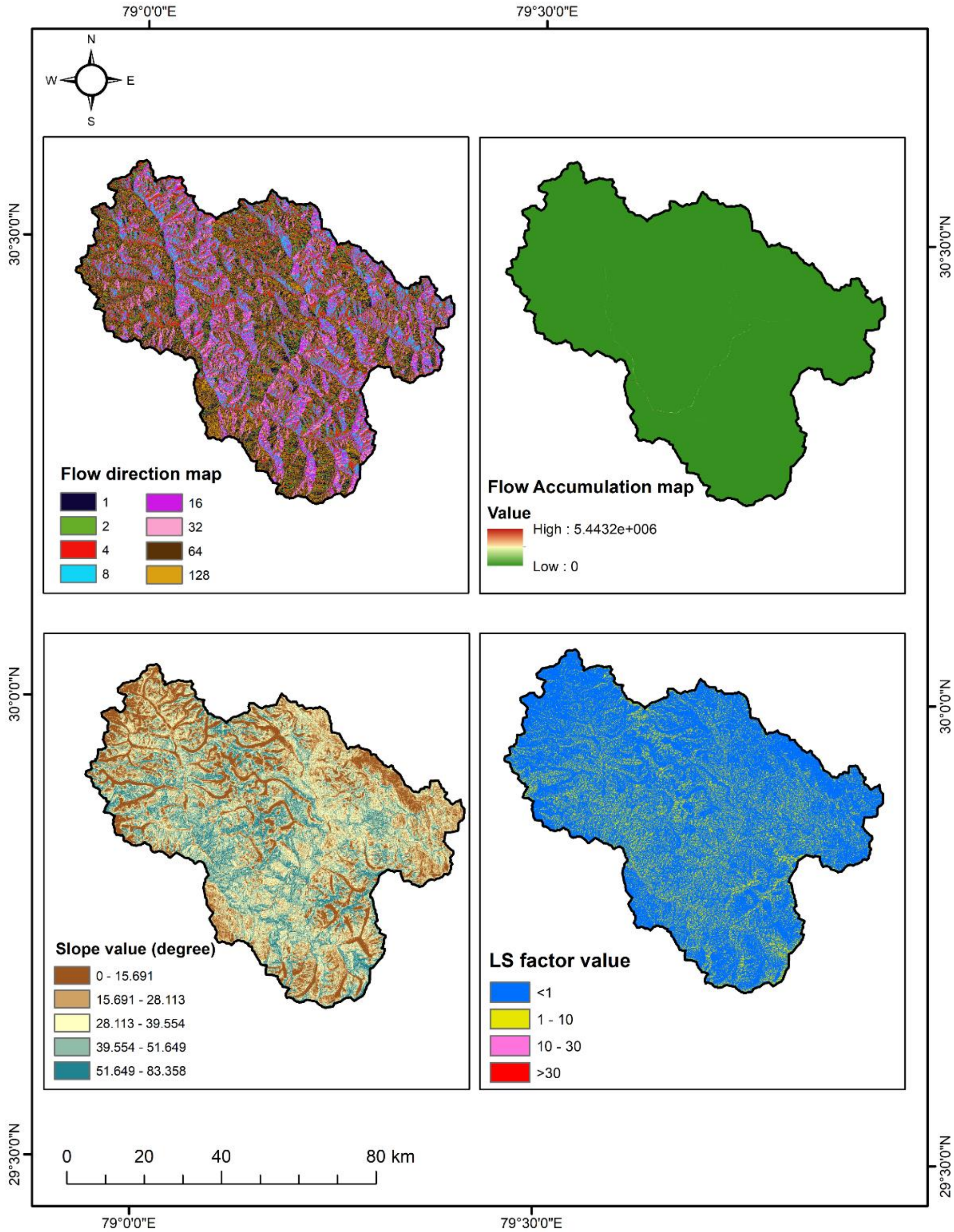

Fig. 5 LS factor map

3.1.5. Support Practice Factor

The determination of P values in the study area was guided by the prevailing LULC classification, given the unavailability of specific support practices. P values were assigned methodically carried out, with land areas depicted on the LULC map receiving a standardized P value of 1. This approach reflects the assumption that these regions do not incorporate specific conservation measures. Conversely, areas characterized by snow/ice cover and water bodies were designated with 0, implying that, devoid of active conservation practices, these features contribute minimally to soil loss control. Figure 7 illustrates the P-factor spatial distribution map, which highlights the absence of control structures, as all land covers are marked green on the legend, representing the highest P value (1). Without implementing control practices in these sensitive land covers and land uses, the basin will likely face increased soil loss soon.

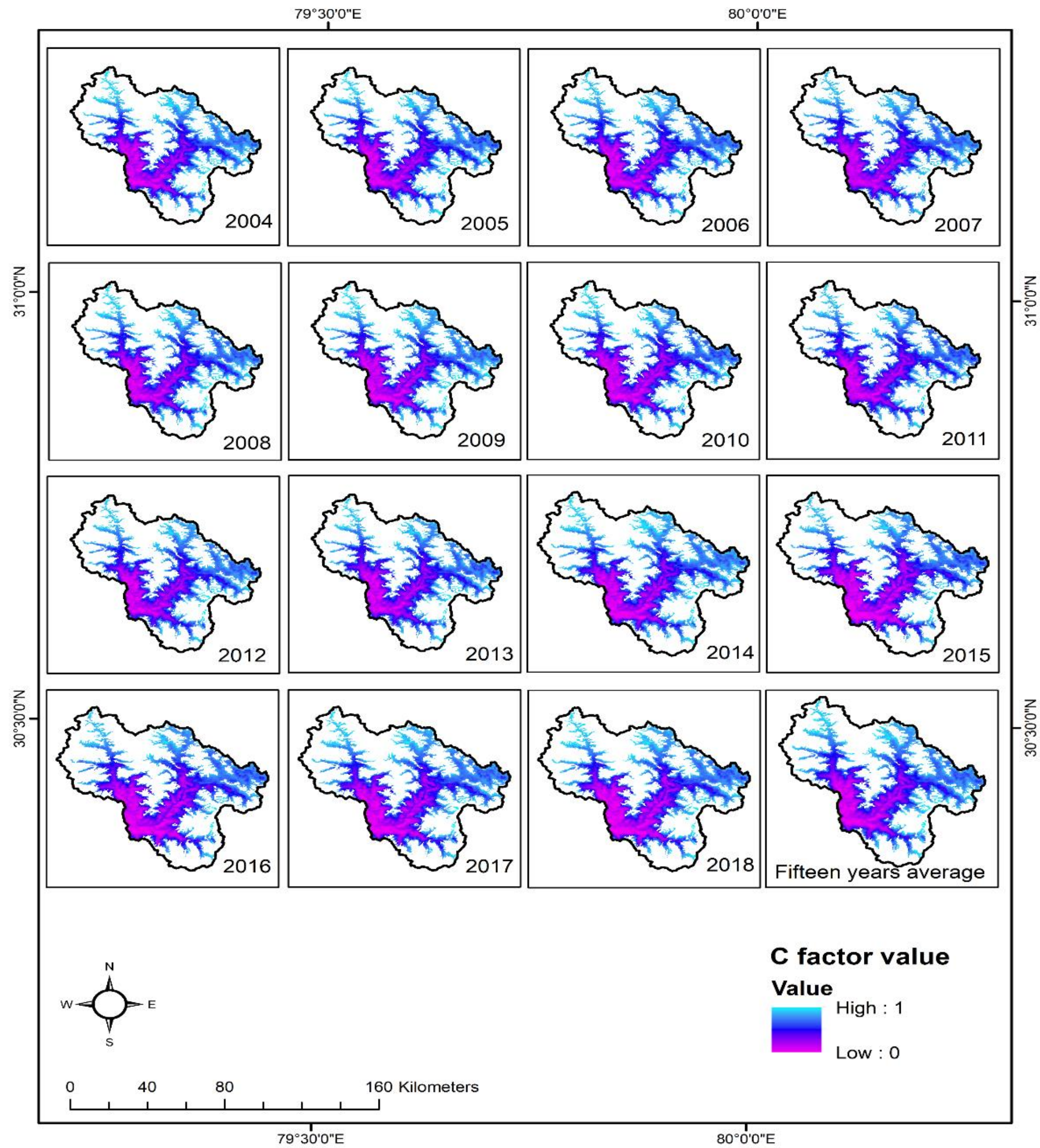

Fig. 6 Average C-factor map; 2004-2018-and fifteen-years average C-factor map

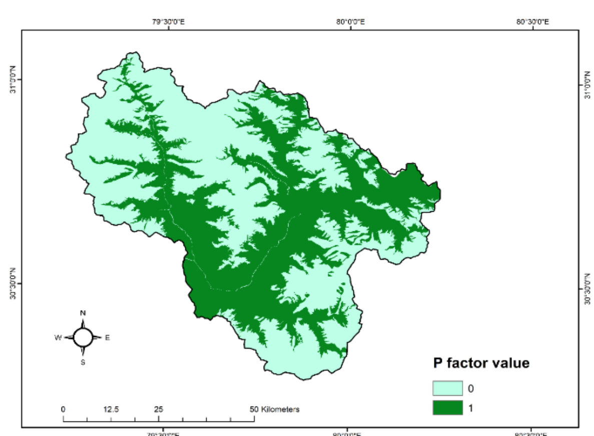

Fig. 7 P-factor map

3.2. Validation

3.2.1. Validation of κ-Factor

The analysis incorporated the 'Soilgrids250m' dataset, encompassing soil depth intervals ranging from 0 to 30 cm to compute soil erodibility factor (κ) employing the equation outlined by Kumar and Hole [10] and Yang et al. [27] serving the purpose of validation.

The resulting average κ value derived from the soil grid was determined to be 0.031 t ha h ha-1 MJ-1 mm-1, closely aligning with the κ value of 0.03 t ha h ha-1 MJ-1 mm-1 calculated from the USDA literature employed in this study.

This good agreement between the calculated and literature values underscores the robust validation of the employed methodology in estimating the κ-factor.

3.2.2. Validation of Ç-Factor

Table 5. C factor comparison among LULC classes

Land Use or Land Cover classes	Ç derived from NDVI (mean)	C from Literature (mean)	Source
Cropland	0.18	0.20	Kumar and Hole (2021)
Grass Land	0.48	0.44	Bhadra et al. (2018)
Built up Land	0.15	0.2	Devatha et al. (2015)
Waste Land	0.65	0.5	Ganasri and Ramesh (2016)
Barren land	0.79	0.75	Nehai et al. (2021)
Evergreen Forest	0.25	0.07	Bhadra et al. (2018)
Shrubland	0.42	0.22	Fu et al. (2005)

The values of Ç acquired for various land classes were compared and validated against reported values from relevant literature. The results revealed a consistent and comparable range between the obtained Ç-factor values and those documented in the literature for corresponding land cover classes. The comparison is presented in Table 5.

3.3. Examining the Spatial Variability in Annual Average Soil Erosion Rates

With a predicted mean soil loss rate of 28.45 t ha−1 yr−1, the Alaknanda River catchment is extremely vulnerable to soil erosion hazards, according to the geographic variation of average annual soil loss analysis. The largest portion of the affected portion falls within the low erosion class at 43.67 % and the smallest portion of the affected area comes within the medium erosion class at 3.78 %. In the spatially distributed layer of the soil loss map, areas under glaciers or without data were excluded as these areas did not significantly impact the overall predicted result. Table 6 displays the percentage of the watershed area categorized under various classes of soil erosion risk.

Table 6. Area under discrete soil erosion classes of alaknanda river basin

Soil Erosion ($t\ ha^{-1}y^{-1}$)	Soil Erosion Class	Percent Area (%)
0-5	Low	43.67
5-10	Medium	3.78
10-20	High	8.40
20-40	Very high	13.80
40-80	Severe	16.39
>80	Very severe	13.93

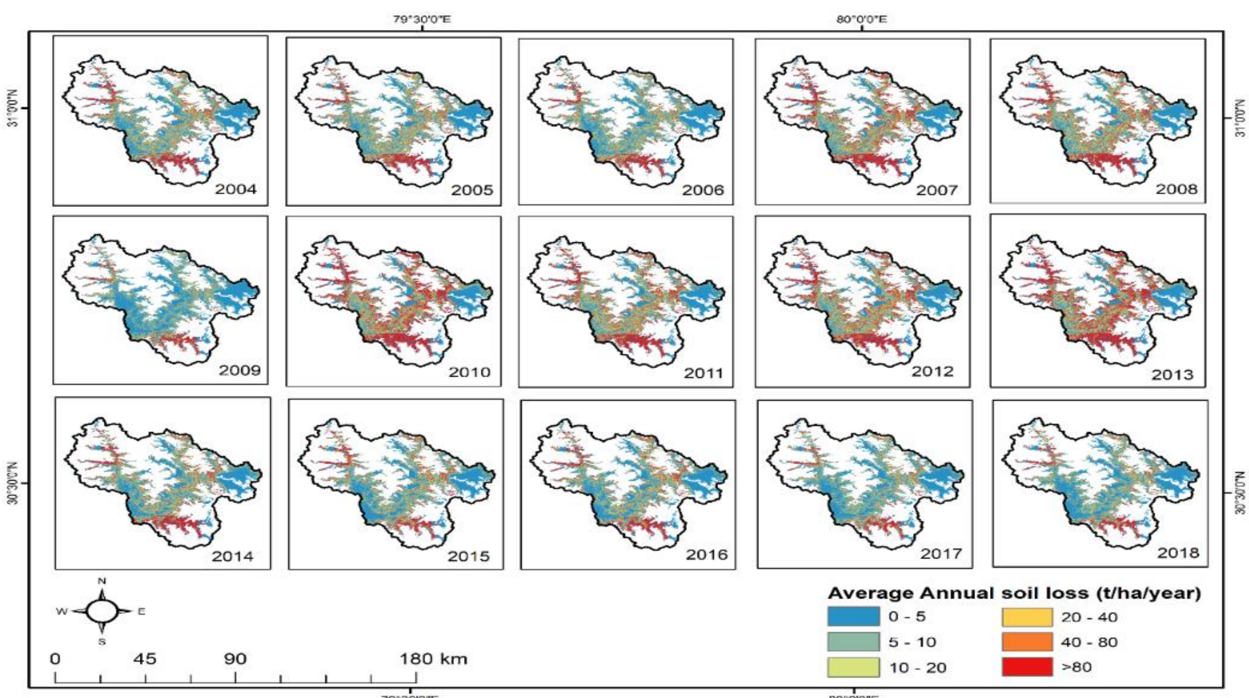

Fig. 8 Annual mean soil erosion map for the consecutive years 2004-2018

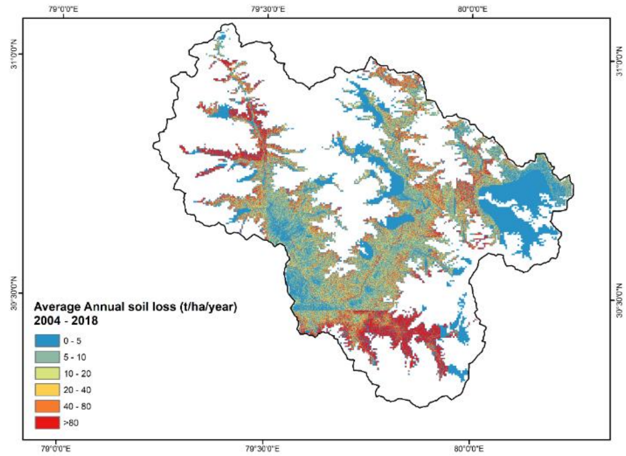

Fig. 9 Mean soil erosion map for the whole study period (2004-2018)

The zonal statistics table, generated by overlaying the mean soil erosion layer with the LULC map, illustrates that areas characterized by barren land, grassland, shrubland, and wasteland exhibit the highest mean soil loss values where among this, the barren land has the maximum value of mean soil loss amount of 26.691 t ha-1 yr-1. Whereas regions classified as built area land and cropland display the minimum value of mean soil loss rates with values of 4.457 and 7.339 t ha-1 yr-1, respectively. The spatial map of the annual mean soil erosion from 2004 to 2018 is represented in Figure 8, while Figure 9 presents the overall average soil erosion map for the same time window.

The Alaknanda basin, situated in the physiographic region of the middle Himalayas, exhibits notably elevated soil erosion rates compared to certain other areas within the state. This heightened erosion is largely attributed to the region's receiving higher rainfall and escalating slope. A comprehensive study conducted by Kumar and Hole [10] encompassing the entire state of Uttarakhand reported a mean soil erosion of about 31.23 t ha^{-1} yr^{-1} for the region of Alaknanda basin. In contrast, Singh and Kansal [21] reported a lower estimate of average soil erosion at 13.4 t ha^{-1} yr^{-1} for the same catchment.

However, their study encompassed a larger coverage area, dividing the watershed into 12 sub-basins named WS1 to WS12, where the maximum mean soil loss measuring up to 27.9 t ha^{-1} yr^{-1} was observed in WS7, a sub-basin that overlaps with the region of our current study. The average soil loss value determined in our present study closely aligns with the findings of Singh and Kansal [21].

In our study, the predicted mean soil loss demonstrated an underestimation compared to the former study but a slight overestimation relative to the latter. This disparity in results may be attributed to variations in dataset types or the watershed size considered in each study. Nevertheless, all these investigations highlight a severe erosion scenario in the Alaknanda basin, emphasizing the imperative need for scrutiny, conservation efforts, and promoting sustainable practices throughout the watershed.

3.4. Examining the Temporal Variability in Annual Average Soil Erosion Rates

The time-based dynamics of soil erosion were scrutinized by assessing variations in factors of R and C, while the remaining factors, namely K, P, and LS, remained static throughout the consecutive analysis interval. The comprehensive temporal fluctuations of mean soil loss over the years of the Alaknanda basin and the corresponding erosion sets are presented in Table 7. The mean annual soil loss value for each year rests within the High to Severe class. The year 2013 had the greatest mean soil loss, at 41.37 t ha^{-1} yr^{-1}, while the year 2009 had the lowest, at 16.63 t ha^{-1} yr^{-1}. The graph was plotted to assess the temporal variation within different soil erosion risk classes between the soil erosion class in percentage and the following years and the overall temporal variation throughout the study instance (Figure 10). A declining trend was observed for the period of 2004 – 2010 and increasing trend from 2010 – 2018 for the soil erosion risk classes of low, medium, high, and very high whereas a contrasting trend was depicted where an increasing trend was observed for the period of 2004 – 2010 and a declining trend from 2010 – 2018 for soil erosion risk classes of severe and very severe. The cumulative temporal fluctuation of the average soil loss in the region depicted an escalating trend from 2004 to 2010, followed by a decreasing trend from 2010 to 2018, as shown in Figure 10. This temporal trend aligns with the pattern of rainfall erosivity, indicating that rainfall erosivity contributes substantially to governing soil erosion within the watershed, as stated by Kumar and Hole [10].

Table 7. Overall temporal variation in mean soil loss

Year	Mean Soil Loss (t $ha^{-1}yr^{-1}$)	Soil Erosion Class
2004	26.11	Very high
2005	26.67	Very high
2006	23.90	Very high
2007	34.59	Very high
2008	32.27	Very high
2009	16.63	High
2010	40.23	Severe
2011	33.00	Very high
2012	35.45	Very high
2013	41.37	Severe

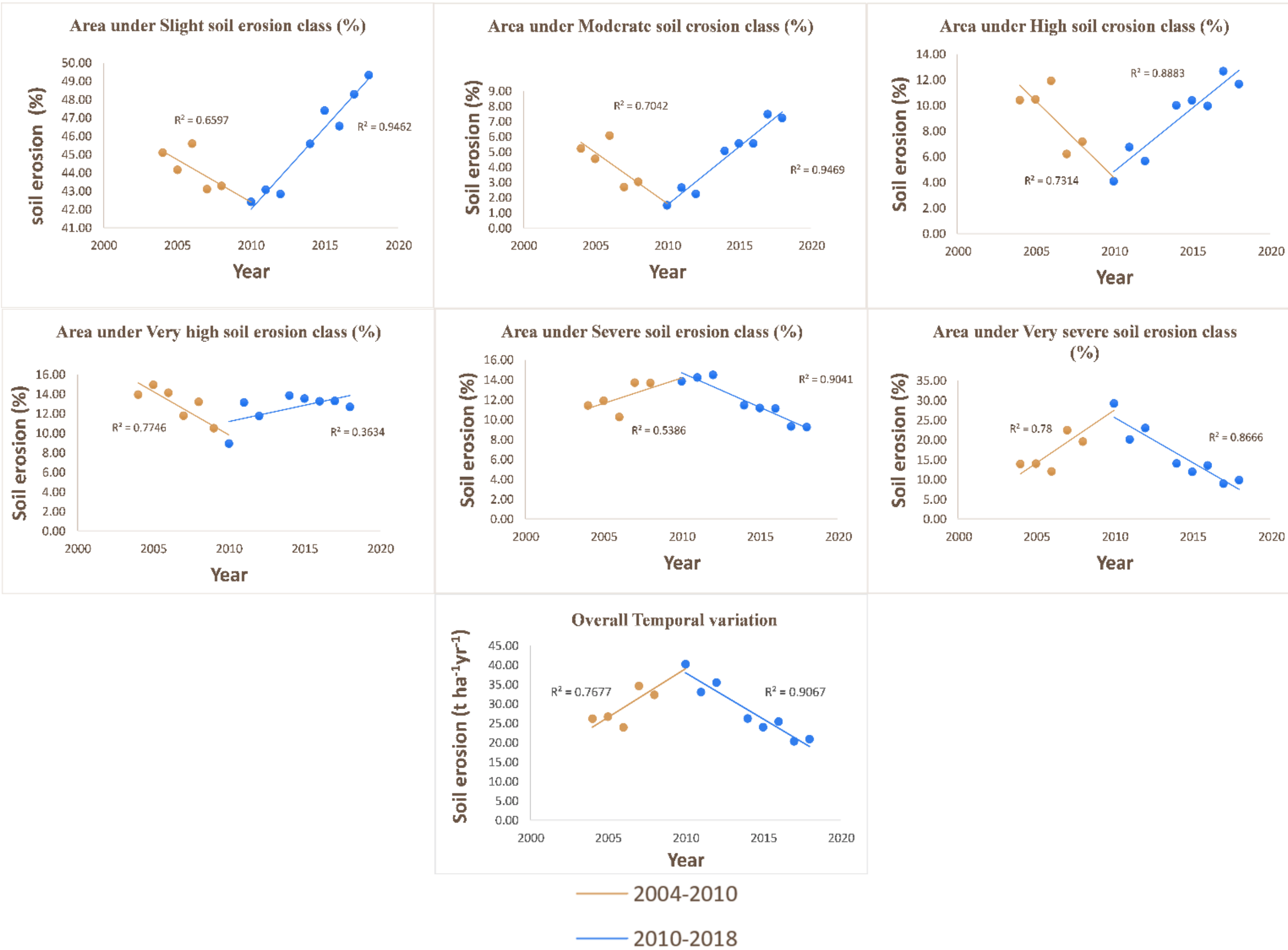

Fig. 10 Temporal variation map for the six classes of soil erosion risk and general temporal variation trend of annual mean soil erosion (2004-2018)

Table 8. Comparative analysis of current work to

Year	**Mean Soil Loss in Alaknanda Basin**	**Mean Soil Loss in Mago Basin**	**Mean Soil Loss in Dibang Basin**	**Mean Soil Loss in Dikrong Basin**
	All Units in (t ha^{-1}yr^{-1})			
2004	26.11	13.33	6.66	43.39
2005	26.67	14.59	3.68	35.22
2006	23.90	5.31	2.84	-
2007	34.59	14.96	4.07	-
2008	32.27	15.26	6.98	-
2009	16.63	22.62	4.87	-
2010	40.23	33.15	8.33	-
2011	33.00	18.41	5.74	-
2012	35.45	20.75	6.49	-
2013	41.37	15.85	4.95	-

'-' indicates no data/no overlapping years between studies

3.5. Comparative Analysis

Table 8 presents a comparative analysis between the current study and previous studies conducted by Dabral et al. [3] which utilized a similar approach to estimate soil loss rates. This comparison highlights the temporal variations in soil erosion. It provides insights into how different study areas-particularly the western Himalayas (Alaknanda), the eastern Himalayas (Mago, Dibang), and the Brahmaputra floodplains (Dikrong) - along with climatic variability and data acquisition, influence the estimated soil loss. The findings can help us understand soil erosion dynamics in these regions, emphasizing the reliability and applicability of the RUSLE model across various regions.

In the distribution of soil erosion classes, low soil erosion (5–10 t ha^{-1} yr^{-1}) was found to dominate the study region, covering 43.67% of the total area, while moderate soil erosion (10–20 t ha^{-1} yr^{-1}) had the least coverage at 3.78% in this study, whereas the previous studies conducted in Uttarakhand state reported that the slight erosion class dominated the region, covering 57.4% of the total area, while the high erosion class had the least coverage at 1.18%. [10] The difference could be present as a result of this study, which primarily concentrates on the Alaknanda basin, while the latter includes other regions as well. Another study carried out in the Dolakha district of Nepal indicated that 70% of the total area was classified under the low erosion division, whereas the high erosion class accounted for only 2.41% of the total area. [23]. The comparison with these studies highlights the dynamic nature of soil erosion patterns, which are influenced by factors such as topography, land use practices, rainfall intensity, and soil properties. These variations emphasize the need for area-specific conservation approaches to relieve soil loss effectively. The present study emphasizes the pressing need for conservation actions to mitigate hazardous consequences in the region. Given its steep slopes and exposure to torrential rainfall, agroforestry and vegetative barriers should be prioritized to reduce sediment transport and surface runoff. Also, bench terracing and contour bunding are essential for stabilizing slopes and preventing excessive soil loss. To ensure the long-term effectiveness of these measures, regular monitoring and maintenance of conservation structures should be encouraged to prolong their lifespan and efficiency.

4. Conclusion

The evaluated soil loss rate (average annual) in Alaknanda was 28.45 t ha-1 yr-1. ‘Low erosion’ was the most prevalent category, while ‘medium erosion’ was the least. The greatest mean soil loss was recorded in the year 2013 with 41.37 t ha-1 yr-1, and the minimum value was recorded in the year 2009 with 16.63 t ha-1 yr-1. The overall temporal fluctuation in soil loss amounts demonstrates a pattern of intensification from 2004 to 2010, followed by a decline from 2010 to 2018. Incorporating geospatial techniques has demonstrated its effectiveness as a valuable tool for examining and prioritizing areas susceptible to soil erosion. This approach also enhances our understanding of the dataset's efficiency and the reliability of various equations employed in estimating each respective factor. A more comprehensive understanding of temporal variation can be achieved by extending the study period to cover a longer duration and to enhance comprehension of soil erosion trends throughout the year and their correlation with RUSLE factors. The RUSLE model indeed offers significant convenience and practicality, particularly in ungauged watersheds where obtaining observed soil loss data is challenging or unfeasible. By utilizing readily available input requirements like rainfall, soil type, land canopy, topography, and land management strategies, the RUSLE model can effectively analyse and prioritize areas prone to severe soil loss or vulnerability. Additionally, the prospect of incorporating future data into the model may be considered. With the availability of various climate projected scenarios making future precipitation data available and the generation of predicted LULC changes and other available inputs, future soil erosion scenarios may be determined as carried out by the author in the Mago basin. Using the climate projected data, near-future, mid-future and far-future soil erosion scenarios may be generated.

Acknowledgments

The authors would like to acknowledge and sincerely thank the organizing committee of the International Conference on Computer-Aided Modeling for the Sustainable Development of Smart Cities (CAMSSC), sponsored by the Anusandhan National Research Foundation (ANRF), held at the Department of Civil Engineering, North Eastern Regional Institute of Science and Technology (NERIST), Nirjuli, Arunachal Pradesh, India, during November 27–30, 2024, for allowing us to present the paper and sponsoring the paper for publication.

References

[1] H.M.J. Arnoldus, “An Approximation of the Rainfall Factor in the Universal Soil Loss Equation,” *CABI Databases*, pp. 127-132, 1980. [Google Scholar] [Publisher Link]

[2] Krishna P. Bhandari, Jagannath Aryal, and Rotchanatch Darnsawasdi, “A Geospatial Approach to Assessing Soil Erosion in a Watershed by Integrating Socio-Economic Determinants and the RUSLE Model,” *Natural Hazards*, vol. 75, pp. 321-342, 2015. [CrossRef] [Google Scholar] [Publisher Link]

[3] P.P. Dabral, Neelakshi Baithuri, and Ashish Pandey, “Soil Erosion Assessment in a Hilly Catchment of North Eastern India Using USLE, GIS and Remote Sensing,” *Water Resources Management*, vol. 22, pp. 1783-1798, 2008. [CrossRef] [Google Scholar] [Publisher Link]

[4] C.P. Devatha, Vaibhav Deshpande, and M.S. Renukaprasad, “Estimation of Soil Loss Using USLE Model for Kulhan Watershed, Chattisgarh-A Case Study,” *Aquatic Procedia*, vol. 4, pp. 1429-1436, 2015. [CrossRef] [Google Scholar] [Publisher Link]

[5] B.J. Fu et al., “Assessment of Soil Erosion at Large Watershed Scale Using RUSLE and GIS: A Case Study in the Loess Plateau of China,” *Land Degradation & Development*, vol. 16, no. 1, pp. 73-85, 2005. [CrossRef] [Google Scholar] [Publisher Link]

[6] B.P. Ganasri, and H. Ramesh, “Assessment of Soil Erosion by RUSLE Model using Remote Sensing and GIS-A Case Study of Nethravathi Basin,” *Geoscience Frontiers*, vol. 7, no. 6, pp. 953-961, 2016. [CrossRef] [Google Scholar] [Publisher Link]

[7] José M. García-Ruiz et al., “A Meta-Analysis of Soil Erosion Rates Across the World,” *Geomorphology*, vol. 239, pp. 160-173, 2015. [CrossRef] [Google Scholar] [Publisher Link]

[8] Mitthan Lal Kansal, and Sachchidanand Singh, “Flood Management Issues in Hilly Regions of Uttarakhand (India) Under Changing Climatic Conditions,” *Water*, vol. 14, no. 12, pp. 1-24, 2022. [CrossRef] [Google Scholar] [Publisher Link]

[9] Christos G. Karydas, Panos Panagos, and Ioannis Z. Gitas, “A Classification of Water Erosion Models According to their Geospatial Characteristics,” *International Journal of Digital Earth*, vol. 7, no. 3, pp. 229-250, 2014. [CrossRef] [Google Scholar] [Publisher Link]

[10] K. Justin George, Suresh Kumar, and Rani M. Hole, “Geospatial Modelling of Soil Erosion and Risk Assessment in Indian Himalayan Region-A Study of Uttarakhand State,” *Environmental Advances*, vol. 4, pp. 1-14, 2021. [CrossRef] [Google Scholar] [Publisher Link]

[11] Deepesh Machiwal, Pratibha Katara, and H.K. Mittal, “Estimation of Soil Erosion and Identification of Critical Areas for Soil Conservation Measures Using RS and GIS-Based Universal Soil Loss Equation,” *Agricultural Research*, vol. 4, pp. 183-195, 2015. [CrossRef] [Google Scholar] [Publisher Link]

[12] W. Maetens et al., “Effects of Land Use on Annual Runoff and Soil Loss in Europe and the Mediterranean: A Meta-Analysis of Plot Data,” *Progress in Physical Geography*, vol. 36, no. 5, pp. 599-653, 2012. [CrossRef] [Google Scholar] [Publisher Link]

[13] Ian D. Moore, and Gordon J. Burch, “Physical Basis of the Length-Slope Factor in the Universal Soil Loss Equation,” *Soil Science Society of America Journal*, vol. 50, no. 5, pp. 1294-1298, 1986. [CrossRef] [Google Scholar] [Publisher Link]

[14] Soumeya Atika Nehai, Mohamed Saïd Guettouche, and Djouher Saadoud, “Regional Modeling of Soil Sensitivity to Water Erosion in JIJEL Region (Algeria) Using MCA and GIS,” *Applied Geomatics*, vol. 13, pp. 55-70, 2021. [CrossRef] [Google Scholar] [Publisher Link]

[15] Panos Panagos et al., “Estimating the Soil Erosion Cover-Management Factor at the European Scale,” *Land Use Policy*, vol. 48, pp. 38-50, 2015. [CrossRef] [Google Scholar] [Publisher Link]

[16] Ashish Pandey, V.M. Chowdary, and B.C. Mal, “Identification of Critical Erosion Prone Areas in the Small Agricultural Watershed Using USLE, GIS and Remote Sensing,” *Water Resources Management*, vol. 21, pp. 729-746, 2007. [CrossRef] [Google Scholar] [Publisher Link]

[17] V. Prasannakumar et al., “Estimation of Soil Erosion Risk within a Small Mountainous Sub-Watershed in Kerala, India, Using Revised Universal Soil Loss Equation (RUSLE) and Geo-Information Technology,” *Geoscience Frontiers*, vol. 3, no. 2, pp. 209-215, 2012. [CrossRef] [Google Scholar] [Publisher Link]

[18] Kenneth G. Renard, *Predicting Soil Erosion by Water: A Guide to Conservation Planning with the Revised Universal Soil Loss Equation (RUSLE)*, U.S. Department of Agriculture, Agricultural Research Service, pp. 1-384, 1997. [Google Scholar] [Publisher Link]

[19] Vishwa N. Sharda, and Prabhat R. Ojasvi, “A Revised Soil Erosion Budget for India: Role of Reservoir Sedimentation and Land-Use Protection Measures,” *Earth Surface Processes and Landforms*, vol. 41, no. 14, pp. 2007-2023, 2016. [CrossRef] [Google Scholar] [Publisher Link]

[20] Gurmel Singh et al., “Soil Erosion Rates in India,” *Journal of Soil and Water Conservation*, vol. 47, no. 1, pp. 97-99, 1992. [Google Scholar] [Publisher Link]

[21] Sachchidanand Singh, and Mitthan Lal Kansal, “Sub-Basin Prioritisation Using RUSLE in a Mountainous River Basin of Uttarakhand (India),” *Environment, Development and Sustainability*, vol. 26, pp. 6851-6877, 2023. [CrossRef] [Google Scholar] [Publisher Link]

[22] *National Soil Survey Handbook*, US Department of Agriculture-Soil Conservation Service, Agriculture 1993. [Google Scholar] [Publisher Link]

[23] Pawan Thapa, “Spatial Estimation of Soil Erosion Using RUSLE Modeling: A Case Study of Dolakha District, Nepal,” *Environmental Systems Research*, vol. 9, no. 1, pp. 1-10, 2020. [CrossRef] [Google Scholar] [Publisher Link]

[24] J.M. van der Knijff, R.J.A. Jones, and L. Montanarella, “*Soil Erosion Risk: Assessment in Europe*,” Report, pp. 1-38, 2000. [Google Scholar] [Publisher Link]

[25] Jing Wang et al., “Analysis of Soil Erosion Characteristics in Small Watershed of the Loess Tableland Plateau of China,” *Ecological Indicators*, vol. 137, pp. 1-12, 2022. [CrossRef] [Google Scholar] [Publisher Link]

[26] Walter H. Wischmeier, and Dwight David Smith, *Predicting Rainfall Erosion Losses: A Guide to Conservation Planning*, Department of Agriculture, Science and Education Administration, pp. 1-58, 1978. [Google Scholar] [Publisher Link]

[27] Yuanyuan Yang et al., “Integrating Multi-Source Data to Improve Water Erosion Mapping in Tibet, China,” *Catena*, vol. 169, pp. 31-45, 2018. [CrossRef] [Google Scholar] [Publisher Link]